Proceedings of ICEGEE 2026 Symposium: Sustainable Environment and Ecology: Supporting a Sustainable Environment for Birds
DOI: 10.54254/2753-8818/2026.BH32614

Comparison of Surface Energy Balance Between Polar Sea Ice and Mid-to-Low Latitude Regions

Jinzhuo Xiang[1*], Linzhuang Yue[2], Chuzhe Feng[3]

[1]Kharkiv Institute, Hangzhou Normal University, Hangzhou, China
[2]Department of Geography, University of Sheffield, Sheffield, United Kingdom
[3]The Affiliated High School of South China Normal University, Guangzhou, China
**Corresponding Author. Email: 01295114@qq.com*

Abstract. The actuality of Earth's Energy Imbalance is extremely associated with global warming and sea level rise, with a more noticeable warming trend being observed in the Arctic region. The aim of this study is to quantify the effects of various climatic factors on radiation at different latitudes in the Northern Hemisphere through the utilization of satellite and reanalysis datasets, in order to recognize the primary driving factors for the situation of global energy imbalance. Through the utilization of the ordinary least squares method and the random forest method, an analysis was conducted of the effects of sea ice concentration, sea surface temperature, cloud cover, atmospheric water vapor, and aerosols on the top-of-atmosphere radiation in the mid-low latitudes (0°-70°N) and high latitudes (70°-90°N) regions. It is indicated by the findings that in the mid-low regions, the main drivers of radiation are identified as cloud cover and aerosols, and in the high-latitude areas, obvious influences on radiation are exerted by the effects of TCC and AOD, but a notable increase is observed in the contribution of TCWV. Meanwhile, a critical role in shortwave radiation and net radiation is also played by sea ice concentration. However, a clear identification of the main driving factors behind the warming trend in the Arctic region is failed to be achieved by the research. The incorporation of more variables related to atmospheric dynamics with a larger time span can be made by future studies, and the time lag effect can be taken into account to better assess the impact of sea ice concentration on radiation.

Keywords: Earth's energy imbalance, Climatic factors, Latitudinal analysis, Regression analysis

1. Introduction

Global warming is the long-time augment in Earth's average surface temperature, mainly driven by human events that strengthen the greenhouse effect [1]. This process is driven by an imbalance of the Earth's energy budget which the amount of absorbed solar radiation exceeds the outward longwave radiation, a persistent net energy accumulation is induced [2,3].

The Earth's top-of-atmosphere (TOA) energy balance depends on both incoming shortwave radiation and outgoing radiation. The outgoing radiation consists of solar radiation reflected by the atmosphere and thermic radiation emitted from the climate system, including the atmosphere [1]. In

DOI: 10.54254/2753-8818/2026.BH32614

principle, the amount of incoming radiation should be equal to outgoing radiation to maintain the overall balanced Earth energy budget and thus the long-term stable global temperature (NASA). An augment in Earth's Energy Imbalance (EEI) at a rate that is much faster than estimated in recent decades has been revealed by satellite and ocean data, specifically energy accumulating in the Earth system, which is associated with climbing global temperatures, elevating sea levels and extreme climate events around the earth [4,5], generally due to enhanced radiation absorbed, with radiation emitted rising to a lesser extent [6]. The trend is particularly pronounced in the Northern Hemisphere, where high latitudes are projected to warm at a rate two to four times faster than the global average. This phenomenon is known as Arctic Amplification [7-9].

Several studies focus on the variation of radiation conditions across latitudes. Zonal means were calculated by Trenberth et al. [10] to outline the latitudinal structure of energy balance, revealing that tropical and subtropical regions exhibit the opposite pattern. This was subsequently expanded upon by research with attempts made to analyze factors accounting for top-of-atmosphere radiation based on latitudinal zonal means calculated from various datasets [11]. However, limitations are that different sources have different data of the same parameter, and reanalyzed data would differ from observed data of variables like aerosols [6,12].

In recent years, the energy budget has been identified as a critical tool for monitoring climatic variation. The mechanisms of solar radiation absorption, reflection, and re-radiation, along with the energy exchange between terrestrial surfaces and the atmosphere, were examined by Trenberth et al. [10]. These analyses were conducted using satellite and reanalysis datasets within a radiation model and land surface model (CLM3) framework. Similarly, the energy balance of the Arctic Ocean was investigated by Trenberth [13] through an integrated energy budget approach. Furthermore, observed sea heat content and climate simulations were assessed by Hansen et al. [14], revealing that more solar energy is currently being absorbed by the Earth than is being emitted as heat, thereby confirming a state of persistent energy imbalance.

With the development of advanced analytical techniques, various drivers of the energy balance have been explored. For instance, cloud cover variations and their impact on the Arctic climate were scrutinized by Beesley [15], where the relationship between radiative forcing and sea ice thickness was modeled through the Single-Column Model (SCM). It was concluded that ice thickness is enhanced by the presence of clouds, with significant seasonal fluctuations being observed. Predictor variables were processed using Partial Least Squares (PLS) regression by Brown and Caldeira [16], with model outputs constrained by CERES observational data. It was subsequently inferred that future global warming may be more severe than previously projected.

The sensitivity of atmospheric energy and wet balances to reductions in Arctic sea ice and ocean warming was studied by David et al. [17] through the utilization of the Weather Research and Forecasting (WRF) model. It was found that significant effects were exerted on local climate by decreasing Arctic sea ice, and the climate in mid-latitude regions was impacted. Satellite observations were combined with CMIP5 climate model simulations by Alkama et al. [18] to examine the relationships between clouds and radiation, and the radiative effects of polar clouds on sea ice changes were quantified, with the critical character of clouds in regulating the polar energy balance being highlighted.

In the studies on the energy budget of the Arctic area and the mid-low latitude regions, the parameterized meridional energy flux (Fwall) [15], the energy budget framework [19], coupled climate models [7], the atmospheric circulation model ECEARTH-IFS [20], and the Rossby stationary wave propagation theory [21] were utilized by scholars to reveal the potential causes of rapid warming and sea ice melting in the Arctic regions from various aspects, and an important

DOI: 10.54254/2753-8818/2026.BH32614

theoretical basis for subsequent research was provided. However, deficiencies have been identified in the study of the combined influence of different factors on the polar regions.

Despite these advancements, several research gaps have been identified. Often, only single factors have been prioritized, leading to a restricted analytical scope. A comprehensive understanding of multi-factor coupling remains elusive, and uncertainty is often compounded by the integration of inconsistent datasets. At present, a lack of discussion on multi-variable radiation influences across different latitude zones has been noted. Consequently, these gaps are addressed in this study through the integration of standardized satellite and reanalysis data. Unlike earlier single-factor analyses, multiple motivations for TOA radiation are considered within a new framework, and new insights into the drivers of Earth's energy imbalance are offered through regression methods such as random forest.

2. Data

2.1. CERES

The CERES Energy Balanced and Filled (EBAF) Ed4.0 product was selected as the source for TOA flux data [22] in this research. This dataset is composed of monthly averages provided at a spatial resolution of 1° × 1°. Global coverage is maintained daily by instruments on the Terra and Aqua satellites, from which mean regional fluxes are derived. Both cloudy and clear-sky conditions are included in the analysis. For regions where cloud-free areas are absent, clear-sky fluxes were estimated based on measurements from CERES and MODIS instruments.

2.2. ERA5

Atmospheric parameters, including Total Cloud Cover, Sea Surface Temperature, Sea Level Pressure, and Water Vapour, were obtained from the ERA5 reanalysis [23]. These records were generated through the integration of observations and model forecasts via the ECMWF IFS CY41R2 system. A resolution of 1° × 1° is possessed by this data.

2.3. Aerosol

Aerosol Optical Depth (AOD) data [24] from MERRA-2 was utilized for this research. This product was developed by NASA's Goddard Space Flight Center through the combination of radiometric, wave, and GPS observations. The production of this data was carried out using the GEOS system (version 5.12.4), and a resolution of 0.5° × 0.625° is featured.

2.4. Sea ice concentration

Sea ice concentration (SIC) data was retrieved from the National Snow and Ice Data Center (NSIDC) [25]. Both daily and monthly SIC records for the polar regions are encompassed by this dataset at a spatial resolution of 25 km × 25 km. Specifically, data from the AMSR2 instrument on the GCOM-W1 satellite was used. Although resampled to 25 km, a highly accurate depiction of ice conditions was ensured by the instrument's high native resolution of 12.5 km × 12.5 km.

DOI: 10.54254/2753-8818/2026.BH32614

2.5. Preprocessing

Monthly averages spanning from January 2020 to December 2024 were covered by the collected data. All parameters were regridded to a standardized 90 × 360 spatial grid. This alignment was achieved through linear or bilinear interpolation, and missing values in the original data were filled using bilinear methods. All variables were calculated as average values based on latitude.

2.6. Study area

The study area was located in the Northern Hemisphere and was partitioned into two regions: the mid-low latitude region (0° -- 70°N) and the high latitude region (70°N -- 90°N). The influences of various climatic factors on TOA radiation (including net, longwave, and shortwave radiation) were investigated within these areas [19,26,27]. This approach followed established methodologies from prior studies on the Arctic energy budget.

3. Method

3.1. Ordinary Least Squares

Ordinary Least Squares (OLS) is a statistical method by which parameters are estimated through linear regression. The relationship between a dependent variable and several independent variables is estimated through the minimization of the total squared differences between the actual and predicted values in the regression model. AOD, SLP, TCC, SST, TCWV, and SIC data are used as independent variables, and multiple linear regression analysis based on the least squares method is conducted with net radiation, longwave radiation, and shortwave radiation as the three dependent variables, whereby the influence of different factors on radiation is preliminarily inferred. The statistical significance of the regression analysis was assessed using a two-tailed t-test [7,26].

$$\sum_{i=0}^{m} (p(x_i) - y_i)^2 = \min$$

where p(x) denotes the expected function that fits the observed data set, with x being the independent variable and y the dependent variable. The corresponding differential equation must be determined [28] to obtain the optimal setting parameters for y=p(x). All processes were carried out using Python in this research.

3.2. Random forest

Random forest is an ensemble learning algorithm that is based on many decision trees. The decision tree is a tree-structure model where each inner node represents a judgment on a characteristic, each branch corresponds to a different result of the judgment, and every leaf node contains a prediction result (such as "yes" or "no") [29]. In this study, the accuracy and stability of the forecasts are enhanced by the random forest method through averaging the results of many decision trees. The independent variables selected are ADO, SLP, TCC, TCWV, SST, and SIC, while the dependent variables are NET, LW, and SW. The importance of each feature will be assessed by considering the contribution made by it to each tree in the random forest.

DOI: 10.54254/2753-8818/2026.BH32614

4. Result

4.1. Result of ordinary least squares method

In mid-low latitude regions (as shown in Fig 1 and Table 1), the primary influences on radiation are AOD and TCC. AOD is significantly positively correlated with shortwave radiation (SW), longwave radiation (LW), and net radiation (NET), indicating that the scattering and absorption capacity of the aerosphere is increased by the presence of aerosols. Regarding SW, while some solar radiation is scattered by aerosols, some solar radiation is also allowed to reach the ground through scattered pathways. By absorbing solar radiation, the atmosphere is heated by aerosols, causing more LW to be emitted toward the ground, thereby increasing the overall NET reaching the ground. Regarding LW, LW emitted by the ground is absorbed by aerosols and then more LW is transmitted toward the ground, whereby atmospheric back-radiation is enhanced and the LW quantity arriving at the land is increased. TCC is significantly negatively correlated with NET, LW, and SW, primarily due to the strong reflective influence of clouds on solar SW, by which a large quantity of solar radiation is reflected back to space and the quantity of solar SW reaching the ground is reduced. At the same time, a strong absorption and scattering effect on long-wave radiation is exerted by clouds. LW from the land is absorbed by them and scattered in all directions, whereby the quantity of LW directly arriving at the land is decreased, thereby reducing the NET.

Table 1. OLS results of radiation affected by different factors at 0-70 degrees

(Coef, t)	Net radiation	Longwave radiation	Shortwave radiation
Total Column Water Vapour	(10.18, 63.80)	(-0.53, -3.9)	(6.38, 55.13)
Total Cloud Cover	(-407.94, -42.19)	(-134.22, -16.4)	(-248.93, -35.49)
Sea Surface Temperature	(-12.82, -48.18)	(0.99, 4.39)	(-11.19, -57.99)
Aerosol Optical Thickness	(611.835, 45.56)	(195.74, 17.22)	(296.34, 30.41)
Sea Level Pressure	(0.03, 13.45)	(-0.01, -5.27)	(0.05, 25.90)

coef: Regression coefficient, representing the independent effect of each independent variable on the dependent variable when all other independent variables are controlled. The t-value represents the regression coefficient divided by the standard error. The smaller the absolute value of the t-value, the less significant the impact of that feature on the dependent variable.

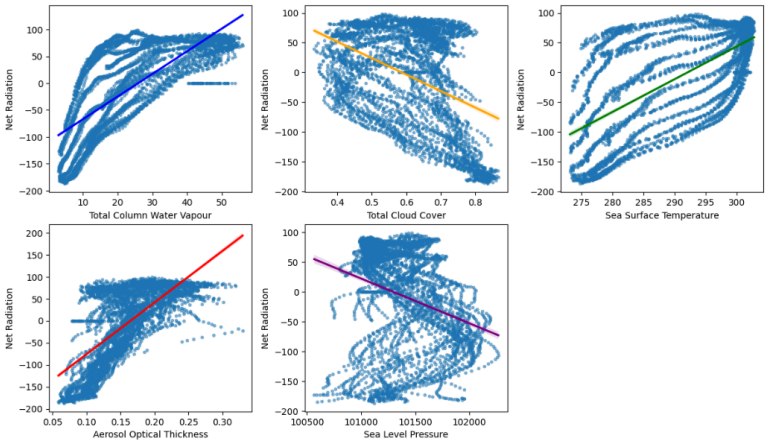

DOI: 10.54254/2753-8818/2026.BH32614

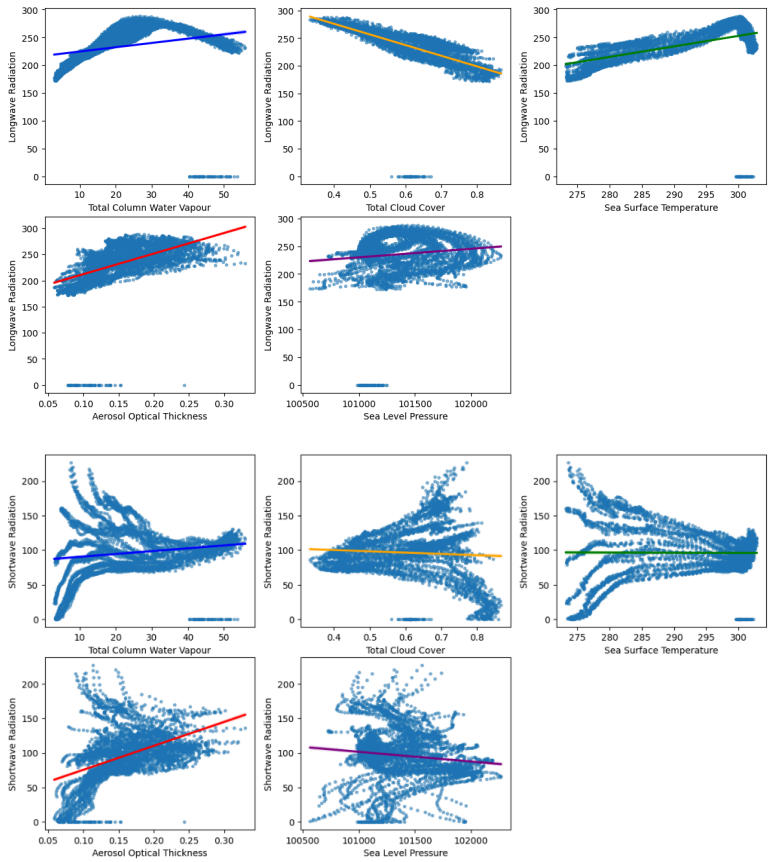

Figure 1. OLS regression results graph of radiation affected by different factors at 0-70 degrees

Radiation dynamics within high-latitude zones (illustrated in Fig 2 and Table 2) were found to be heavily governed by Total Cloud Cover (TCC) and Aerosol Optical Depth (AOD). Observed reductions in NET and SW were tied to rising TCC, while a simultaneous increase in LW was recorded. Variations in cloud structure and composition at high latitudes were identified as factors leading to diminished longwave scattering and augmented absorption relative to mid-low latitude regions. Consequently, after LW emitted from the surface is trapped by clouds, a larger proportion is redirected toward the ground, thereby bolstering the LW flux reaching the surface. Nevertheless, the influence exerted on net and shortwave radiation remained predominantly linked to the reflection of solar radiation by cloud cover.

Strong positive correlations were established between AOD and the variables NET, LW, and SW. A more intensified greenhouse effect was exerted by high-latitude aerosols, allowing longwave radiation to be more efficiently captured and re-emitted. Atmospheric scattering and solar absorption were consequently enhanced, and the ground was further insulated, resulting in elevated surface levels of NET, LW, and SW.

Regarding Sea Ice Concentration (SIC), upward trends in SW and NET were documented in response to declining ice levels. This phenomenon was primarily attributed to the high albedo of sea ice, which serves as a potent reflector of short-wave solar radiation. A substantial portion of solar radiation was redirected back to space through this mechanism, whereby the energy received by the Earth was notably diminished, and a reduction in NET was induced. Although some LW was also reflected by sea ice, the impact on this radiation type was found to be more pronounced, yielding a significant negative effect.

DOI: 10.54254/2753-8818/2026.BH32614

Table 2. OLS results of radiation affected by different factors at 70-90 degrees

(Coef, t)	Net radiation	Longwave radiation	Shortwave radiation
Sea Ice Concentration	(112.98, 7.01)	(-4.40, -1.08)	(102.26, 18.17)
Total Column Water Vapour	(13,57, 27.98)	(4.77, 38.86)	(20.19, 36.90)
Total Cloud Cover	(-328.98, -9.52)	(11.82, 1.35)	(-676.31, -17.36)
Sea Surface Temperature	(0.52, 0.17)	(-2.91, -3.75)	(-17.62, -5.09)
Aerosol Optical Thickness	(446.88, 8.90)	(64.64, 5.09)	(596.26, 10.53)
Sea Level Pressure	(0.01,2.39)	(0.01, 5.87)	(0.01, 2.33)

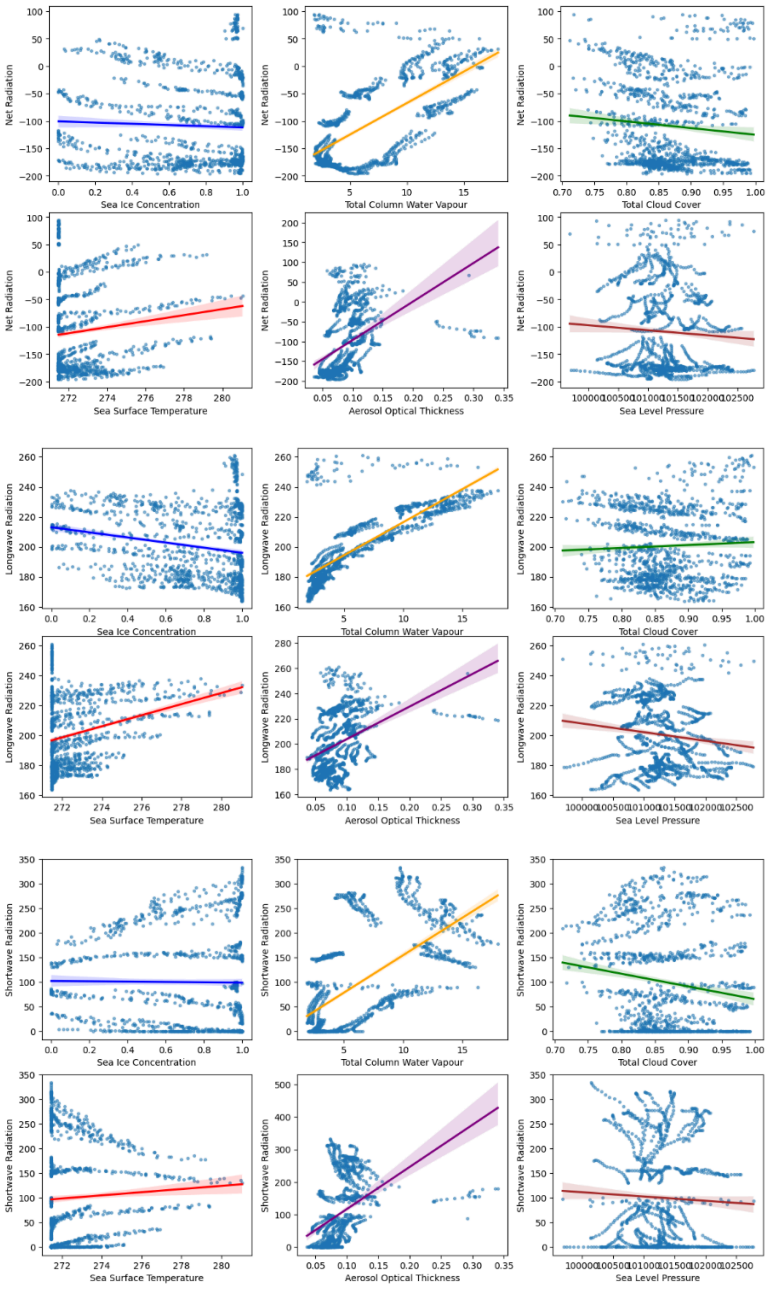

Figure 2. The OLS regression results graph of radiation affected by different factors at 70-90 degrees

DOI: 10.54254/2753-8818/2026.BH32614

4.2. Results of the random forest

Within the mid-low latitude zones (as illustrated in Fig 3), a predominant influence on net radiation was exerted by water vapor, which accounted for a contribution of approximately 60%. This dominance was likely necessitated by the elevated moisture levels characteristic of these regions, through which solar radiation scattering and absorption were intensified, thereby fundamentally defining the net radiation balance. In comparison, substantially smaller roles were played by other variables, including AOD and TCC. Conversely, in high-latitude regions, AOD was identified as the most significant driver, followed closely by water vapor; their combined contribution was found to constitute roughly 40%. A notable impact was also documented for SIC, which accounted for approximately 10% of the variance, thereby emphasizing the heightened importance of aerosols, moisture, and sea ice presence within these colder environments.

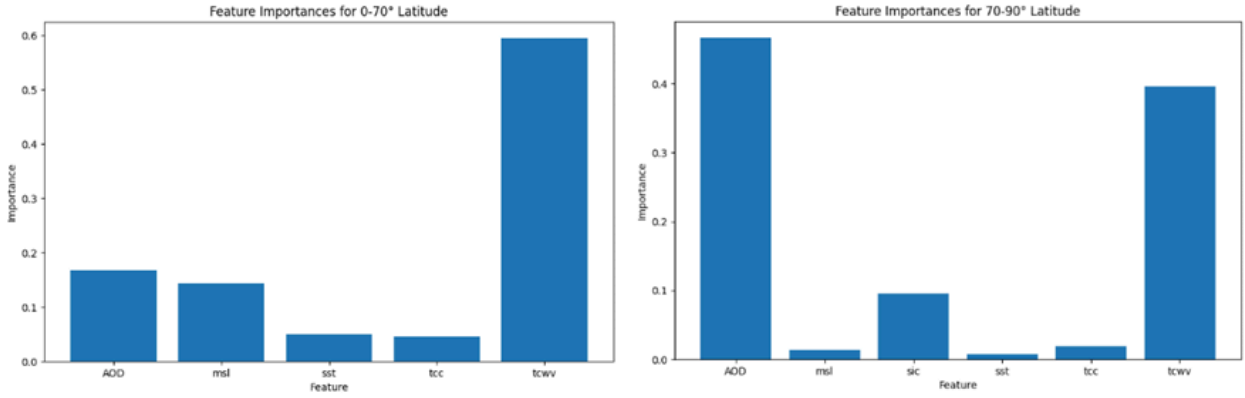

Figure 3. The characteristic importance map of net radiation (RF) due to different factors, with the left side covering 0-70 and the right side covering 70-90

In mid-low latitude zones (as depicted in Fig 4), a 50% contribution to the long-wave radiation balance was attributed to TCC. The essential function of clouds in trapping and re-emitting terrestrial and atmospheric radiation was highlighted by these results, as the propagation and distribution of long-wave radiation were significantly governed by this process. Moderate importance was also assigned to AOD and TCWV, with each representing about 20% of the importance, while relatively negligible contributions were made by SLP and SST. Within high-latitude areas, a sharp escalation in the influence of water vapor on long-wave radiation was observed, reaching nearly 70%. It was suggested by this trend that radiation patterns in these frigid regions are more acutely susceptible to fluctuations in atmospheric moisture. Meanwhile, a decline in the impact of cloud cover was recorded, though contributions of approximately 20% were maintained by both AOD and SIC. It was indicated by these findings that the reflection and absorption effects associated with sea ice become particularly relevant in high-latitude zones characterized by extensive ice cover.

DOI: 10.54254/2753-8818/2026.BH32614

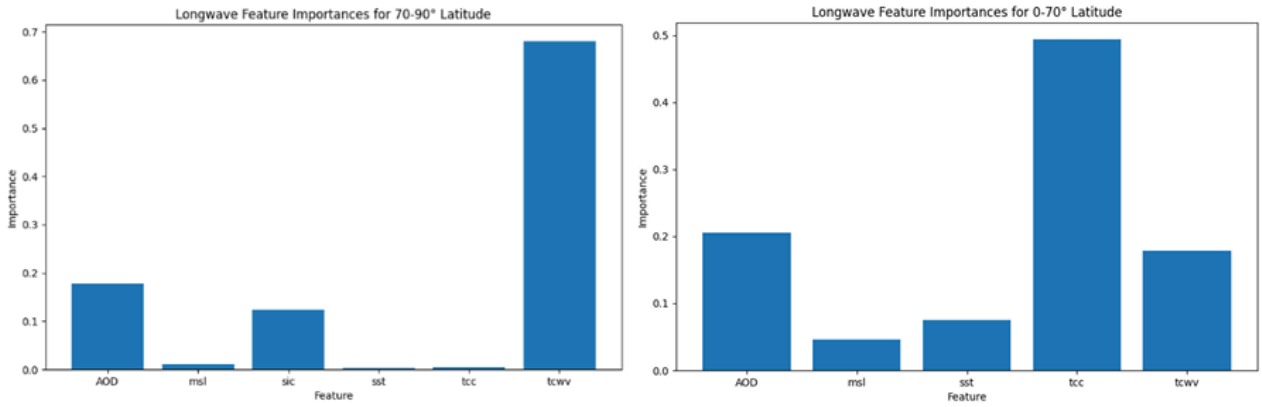

Figure 4. The importance map of different factors for the characteristics of long-wave radiation (RF), with the left side covering 0-70 and the right side covering 70-90

In mid-low latitude regions (as shown in Fig 5), the primary role in shortwave radiation was occupied by AOD, with a contribution of roughly 35%. Shortwave levels were considerably modulated by aerosols via the dual mechanisms of sunlight scattering and absorption—while solar energy reaching the surface was curtailed by scattering, energy levels within the atmosphere were bolstered by absorption. Contributions of approximately 20% were recorded for SST, TCC, and TCWV each, as the thermal structure and radiation transmission of the atmosphere were primarily dictated by these factors. In contrast, within high-latitude areas, a sharp rise in the importance of water vapor content was noted, accounting for approximately 50% of the importance, while a steady contribution of roughly 30% was sustained by AOD. Growth in the relative share of SIC was also observed, reaching nearly 10%. Meanwhile, significantly lower impacts were exhibited by SLP, SST, and TCC, reflecting their diminished influence on shortwave radiation in colder climates.

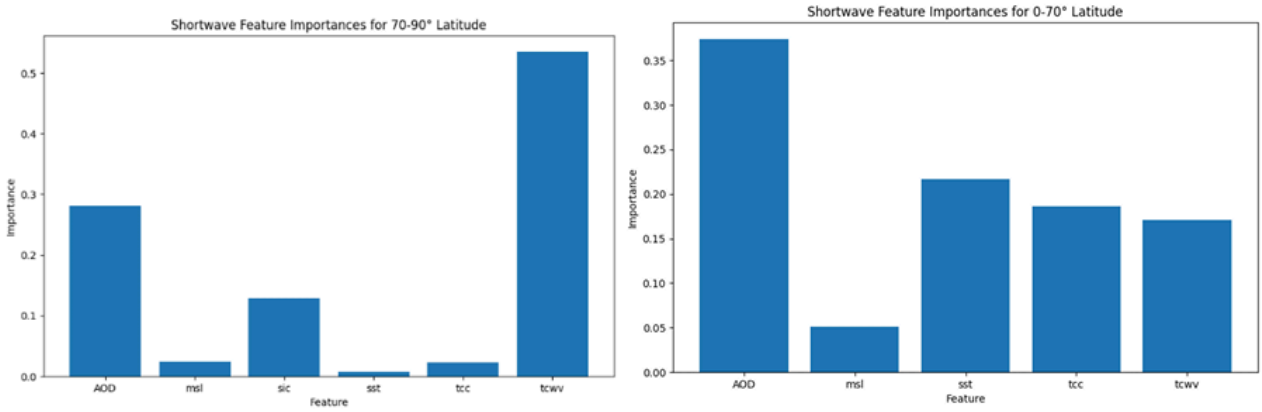

Figure 5. The importance map of different factors for the characteristics of short-wave radiation (RF), with the left side covering 0-70 and the right side covering 70-90

5. Discussion

Within mid-low latitude areas, the reduction of long-wave radiation by TCC was demonstrated by both the OLS and random forest models. Important impacts on long-wave radiation are also exerted by AOD and TCWV. Regarding short-wave radiation (SW), the largest effect is produced by AOD. Smaller effects are exhibited by TCC and TCWV in comparison. Net radiation is mostly influenced by TCWV. In the random forest model, about 60% of the effect is accounted for by TCWV. It is

DOI: 10.54254/2753-8818/2026.BH32614

shown by these findings that in these regions, LW and SW are mainly affected by cloud cover and aerosols. Net radiation is mainly impacted by water vapor content.

In high-latitude regions, consistent results are produced by both models. Strong effects on long-wave radiation remain exerted by TCC and AOD. An increase to about 70% is observed in TCWV's effect. Regarding short-wave radiation, a rise to around 50% is observed in TCWV's influence. AOD's effect stays near 30%, and an influence of about 10% is exhibited by SIC. Net radiation here is mainly affected by AOD and TCWV, which make up about 40% of the total effect in the RF model. An impact of around 10% is exerted by SIC. It is shown by these results that in high-latitude areas, radiation is still influenced by water vapor and aerosols. Importance is also attached to the effect of sea ice concentration on short-wave and net radiation.

Strong influences on net and short-wave radiation in high-latitude areas are exerted by SIC. This is because sunlight is reflected by sea ice. An increase in reflection is caused by covering snow and ice, by which the quantity of solar radiation arriving at the land is decreased. A lowering of net radiation is induced by this.

6. Conclusion

The energy budget in the Northern Hemisphere was analyzed by latitude, and three main points were found. Firstly, in mid- and low-latitude areas, long-wave and short-wave radiation are mainly influenced by TCC and AOD. Net radiation is mainly affected by TCWV. Secondly, in high-latitude areas, radiation is still affected by TCWV and AOD. Considerable influences on SW and NET are exerted by SIC. Thirdly, in high-latitude areas, radiation is impacted by sea ice through reflection. It is shown by our analysis that small effects on all radiation types are produced by SLP. This might be because enough atmospheric variables were not included. Factors like wind speed, wind direction, and atmospheric circulation should be included by future studies for better results.

In high-latitude regions, small effects on LW and lesser effects on SW and NET are exhibited by SIC. This could be because a stable level has been reached by sea ice. Immediate effects on radiation may not be produced by changes in sea ice. Time might be taken to influence radiation. Time lag variables should be added by future research to better understand these effects.

RF and OLS models were used in this study. Limits in handling complex nonlinear relationships are possessed by these models. Advanced machine learning methods like neural networks can be used by future work. Complex links between variables can be better found by these methods.

References

[1] IPCC, 2021: Climate Change 2021: The Physical Science Basis. Contribution of Working Group I to the Sixth Assessment Report of the Intergovernmental Panel on Climate Change [Masson-Delmotte, V., P. Zhai, A. Pirani, S.L.Connors, C. Péan, S. Berger, N. Caud, Y. Chen, L. Goldfarb, M.I. Gomis, M. Huang, K. Leitzell, E. Lonnoy, J.B.R.Matthews, T.K. Maycock, T. Waterfield, O. Yelekçi, R. Yu, and B. Zhou (eds.)]. Cambridge University Press, Cambridge, United Kingdom and New York, NY, USA, 2391 pp. doi: 10.1017/9781009157896

[2] NASA Earth Observatory. (n.d.). Earth's energy balance. NASA. https: //mynasadata.larc.nasa.gov/basic-page/earths-energy-budget

[3] Hansen, J., Nazarenko, L., Ruedy, R., Sato, M., Willis, J., Del Genio, A., ... & Tausnev, N. (2005). Earth's energy imbalance: Confirmation and implications. science, 308(5727), 1431-1435.DOI: 10.1126/science.1110252

[4] Liu, C., Allan, R. P., Mayer, M., Hyder, P., Desbruyères, D., Cheng, L., Xu, J., Xu, F., & Zhang, Y. (2020). Variability in the global energy budget and transports 1985–2017. Climate Dynamics, 55(11–12), 3381–3396. https: //doi.org/10.1007/s00382-020-05451-8

[5] Mauritsen, T., Tsushima, Y., Meyssignac, B., Loeb, N. G., Hakuba, M., Pilewskie, P., Cole, J., Suzuki, K., Ackerman, T. P., Allan, R. P., Andrews, T., Bender, F. A.-M., Bloch-Johnson, J., Bodas-Salcedo, A., Brookshaw, A.,

DOI: 10.54254/2753-8818/2026.BH32614

Ceppi, P., Clerbaux, N., Dessler, A. E., Donohoe, A., & Dufresne, J. (2025). Earth's energy imbalance more than doubled in recent decades. AGU Advances, 6(3), e2024AV001636. https: //doi.org/10.1029/2024AV001636

[6] Loeb, N. G., Ham, S.-H., Allan, R. P., Thorsen, T. J., Meyssignac, B., Kato, S., Johnson, G. C., & Lyman, J. M. (2024). Observational assessment of changes in Earth's energy imbalance since 2000. Surveys in Geophysics, 45(6), 1757–1783. https: //doi.org/10.1007/s10712-024-09838-8

[7] Cohen, J., Screen, J., Furtado, J., Barlow, M., Whittleston, D., Coumou, D., Francis, J., Dethloff, K., Entekhabi, D., Overland, J., & Jones, J. (2014). Recent Arctic amplification and extreme mid-latitude weather. Nature Geoscience, 7(9), 627–637. https: //doi.org/10.1038/ngeo2234

[8] Screen, J. A., & Francis, J. A. (2016). Contribution of sea-ice loss to Arctic amplification is regulated by Pacific Ocean decadal variability. Nature Climate Change, 6, 856–860.

[9] Allan, Richard P., Paola A. Arias, Sophie Berger, Josep G. Canadell, Christophe Cassou, Deliang Chen, Annalisa Cherchi et al. "Intergovernmental panel on climate change (IPCC). Summary for policymakers." In Climate change 2021: The physical science basis. Contribution of working group I to the sixth assessment report of the intergovernmental panel on climate change, pp. 3-32. Cambridge University Press, 2023.

[10] Trenberth, K. E., Fasullo, J. T., & Kiehl, J. (2009). Earth's Global Energy Budget. Bulletin of the American Meteorological Society, 90(3), 311–324. https: //doi.org/10.1175/2008bams2634.1

[11] Hong, Y., Liu, G., & Li, J.-L. F. (2016). Assessing the radiative effects of global ice clouds based on CloudSat and CALIPSO measurements. Journal of Climate, 29(21), 7651–7674. https: //doi.org/10.1175/JCLI-D-15-0799.1

[12] Kato, S., Rose, F. G., Sun-Mack, S., Miller, W. L., Chen, Y., Rutan, D. A., Stephens, G. L., Loeb, N. G., Minnis, P., Wielicki, B. A., Winker, D. M., Charlock, T. P., Stackhouse, P. W., Xu, K.-M., & Collins, W. J. (2011). Improvements of top-of-atmosphere and surface irradiance computations with CALIPSO-, CloudSat-, and MODIS-derived cloud and aerosol properties. Journal of Geophysical Research, 116(D19). https: //doi.org/10.1029/2011jd016050

[13] Trenberth, K. (2007). The large-scale energy budget of the Arctic. Journal of Geophysical Research. https: //doi.org/10.1029/2006JD008230

[14] Hansen, J., Sato, M., Kharecha, P., & von Schuckmann, K. (2011). Earth's energy imbalance and implications. Atmospheric Chemistry and Physics, 11, 13421–13449. https: //doi.org/10.5194/acp-11-13421-2011

[15] Beesley, J. A. (2000). Estimating the effect of clouds on the Arctic surface energy budget. Journal of Geophysical Research: Atmospheres, 105(D8), 10103–10117. https: //doi.org/10.1029/2000jd900043

[16] Brown, P. T., & Caldeira, K. (2017). Greater future global warming inferred from Earth's recent energy budget. Nature, 552(7683), 45–50. https: //doi.org/10.1038/nature24672

[17] Porter, D. F., Cassano, J. J., & Serreze, M. C. (2012). Local and large-scale atmospheric responses to reduced Arctic sea ice and ocean warming in the WRF model. Journal of Geophysical Research, 117(D11). https: //doi.org/10.1029/2011jd016969

[18] Alkama, R., Taylor, P. C., Garcia-San Martin, L., Douville, H., Duveiller, G., Forzieri, G., Swingedouw, D., & Cescatti, A. (2020). Clouds damp the radiative impacts of polar sea ice loss. The Cryosphere, 14(8), 2673–2686. https: //doi.org/10.5194/tc-14-2673-2020

[19] Porter, D. (2010). New estimates of the large-scale Arctic atmospheric energy budget. Journal of Geophysical Research. https: //doi.org/10.1029/2009JD012653

[20] Semmler, T., McGrath, R. & Wang, S. The impact of Arctic sea ice on the Arctic energy budget and on the climate of the Northern mid-latitudes. Clim Dyn 39, 2675–2694 (2012). https: //doi.org/10.1007/s00382-012-1353-9

[21] Rudeva, I., & Simmonds, I. (2021). Midlatitude winter extreme temperature events and connections with anomalies in the Arctic and tropics. Journal of Climate, 34(10). https: //doi.org/10.1175/JCLI-D-20-0371.1

[22] Loeb, N. G., Doelling, D. R., Wang, H., Su, W., Nguyen, C., Corbett, J. G., Liang, L., Mitrescu, C., Rose, F. G., & Kato, S. (2018). Clouds and the Earth's Radiant Energy System (CERES) Energy Balanced and Filled (EBAF) Top-of-Atmosphere (TOA) Edition-4.0 Data Product. Journal of Climate, 31(2), 895–918. https: //doi.org/10.1175/jcli-d-17-0208.1

[23] Hersbach, H., Bell, B., Berrisford, P., Biavati, G., Horányi, A., Muñoz Sabater, J., Nicolas, J., Peubey, C., Radu, R., Rozum, I., Schepers, D., Simmons, A., Soci, C., Dee, D., Thépaut, J-N. (2023): ERA5 monthly averaged data on single levels from 1940 to present. Copernicus Climate Change Service (C3S) Climate Data Store (CDS), DOI: 10.24381/cds.f17050d7

[24] Global Modeling and Assimilation Office (GMAO) (2015), inst3_3d_asm_Cp: MERRA-2 3D IAU State, Meteorology Instantaneous 3-hourly (p-coord, 0.625x0.5L42), version 5.12.4, Greenbelt, MD, USA: Goddard Space Flight Center Distributed Active Archive Center (GSFC DAAC), Accessed Enter User Data Access Date at doi: 10.5067/VJAFPLI1CSIV

DOI: 10.54254/2753-8818/2026.BH32614

[25] Meier, W. N., Fetterer, F., Windnagel, A. K., Stewart, J. S. & Stafford, T. (2024). NOAA/NSIDC Climate Data Record of Passive Microwave Sea Ice Concentration. (G02202, Version 5). [Data Set]. Boulder, Colorado USA. National Snow and Ice Data Center. https: //doi.org/10.7265/rjzb-pf78. Date Accessed 08-30-2025.
[26] Screen, J., & Simmonds, I. (2010). The central role of diminishing sea ice in recent Arctic temperature amplification. Nature, 464(7293), 1334-1337. https: //doi.org/10.1038/nature09051
[27] Semmler, T., Jacob, D., Schlünzen, K. H., & Podzun, R. (2005). The Water and Energy Budget of the Arctic Atmosphere. Journal of Climate, 18(13), 2515-2530. https: //doi.org/10.1175/JCLI3414.1
[28] Pan, T., Wu, S., Dai, E., & Liu, Y. (2013). Estimating the daily global solar radiation spatial distribution from diurnal temperature ranges over the Tibetan Plateau in China. Applied Energy, 107, 384-393. https: //doi.org/10.1016/j.apenergy.2013.02.053
[29] Han, J., Pei, J., & Kamber, M. (2011). *Data Mining: Concepts and Techniques* (3rd ed.). Morgan Kaufmann.